if the condensed monomer film is exposed to ultraviolet light (Day & Lando, 1980). It may be possible to carry out the polymerization within a confined space (Rybnikar *et al.*, 1994) or in dilute solution (Liu & Geil, 1993) to form crystals suitable for electron diffraction data collection. In the latter case, whisker formation with the chain axis parallel to the lath plane has been observed. Films can be cast on a water surface by evaporation of an organic solvent from a polymer solution. The film can then be stretched to give a suitably oriented specimen for data collection (Vainshtein & Tatarinova, 1967). In addition, it may just be possible to obtain suitable data from drawn microfibres to supplement the single-crystal diffraction information from other preparations.

Data collection from these thin microcrystals often employs the selected-area diffraction technique in the electron microscope that is described in detail elsewhere (Dorset, 1995*b*). Using an approximately eucentric goniometric tilting device in the electron microscope, the sampling of three-dimensional reciprocal space is tomographic, *i.e.* the tilts of a nearly planar Ewald sphere surface (owing to the very small electron wavelength) are always referred to a set of reciprocal axes that intersect (0, 0, 0). For any given crystal habit, there is always a missing set of data owing to the physical limitation to the tilt imposed by the finite thickness of the specimen holder within the pole-piece gap of the electron microscope objective lens (Vainshtein, 1964). For this reason, it is desirable to crystallize two orthogonal orientations of the chain packing (using the above-mentioned approaches), if possible, so that all of the reciprocal lattice can be sampled. If electron micrographs are to be used as an additional source of crystallographic phases then 'low-dose' techniques for recording such images should be employed to reduce the deleterious effects of radiation damage caused by the inelastic interactions of the electron beam with the crystalline sample (Tsuji, 1989).

When the diffraction patterns are recorded on photographic film and these are then measured with a densitometer, relative reflection intensities can often be expressed simply as the integrated peak area without need for a Lorentz correction (Dorset, 1995*b*). Only if the diffraction maxima are extensively arced (*e.g.* in patterns from epitaxic films) is such a correction required. That is to say, $|\Phi_{\rm obs}| \propto KI_{\rm obs}^{1/2}$ where $|\Phi_{\rm obs}|$ is the observed structure-factor magnitude. Assuming the kinematical approximation holds, the calculated value is

$$\Phi_h^{\rm calc} = \sum_i f_i \exp 2\pi i(\mathbf{h}\cdot\mathbf{r}),$$

where f_i are the electron scattering factors (Doyle & Turner, 1968), *e.g.* as tabulated in Table 4.3.1.1 in *IT* C. By analogy with X-ray crystallography (see Chapter 2.2), normalized values can be found from

$$|E_h|^2 = I_h^{\rm obs}/\varepsilon\sum_i f_i^2,$$

with the usual scaling condition that $\langle E_h^2\rangle = 1.000$. [Note, however, that these intensities only describe the chain monomer packing in the 'stem' region of the lamellar microcrystal. Details owing to the surface chain folds are lost (even if they are strictly periodic), because of reasons similar to those described by Cowley (1961) for the electron scattering from elastically bent silicate crystals.]

4.5.3.3. Crystal structure analysis

Two approaches to crystal structure analysis are generally employed in polymer electron crystallography. As already mentioned, the procedure adapted from fibre X-ray crystallography relies on the construction of a model (Brisse, 1989; Perez & Chanzy, 1989). Conformational searches (Campbell Smith & Arnott, 1978) simultaneously minimize the fit of observed diffraction data to calculated values (the *R* factor based on structure factors computed *via* known atomic scattering factors) and a nonbonded atom–atom potential function (Tadokoro, 1979). Reviews of structures solved by this approach have been published (Dorset, 1989, 1995*b*).

Recently, direct phasing methods of the kind used in X-ray crystallography (Chapter 2.2 and, applied to electron diffraction, Section 2.5.8) have also been found to be particularly effective for electron crystallographic structure analyses (Dorset, 1995*b*). While the Fourier transform of an electron micrograph would be the most easily imagined direct method, yielding crystallographic phases after image analysis (see Section 2.5.5), this use of micrographs has been of less importance to polymer crystallography than it has been in the study of globular proteins, even though there is at least one notable example where it has been helpful (Isoda *et al.*, 1983*a*) for the determination of a structure from X-ray fibre data. On the other hand, high-resolution images of polymer crystals are of considerable use for the characterization of packing defects (Isoda *et al.*, 1983*b*).

In polymer electron crystallography, the sole reliance on the diffraction intensities for structure analysis has proven, in recent years, to be quite effective. Several direct-methods approaches have been pursued, including the use of probabilistic techniques, either in the symbolic addition procedure, or in more automated procedures involving the tangent formula (see Chapter 2.2). The Sayre (1952) equation has been found to be particularly effective, where the correct structure is identified *via* some figure of merit after algebraic phase values are used to generate multiple solutions (Stanley, 1986). More recently, maximum-entropy and likelihood methods (Gilmore *et al.*, 1993) have also been effective for solving such structures. After the initial atomic model is found, it can be improved by refinement, generally using Fourier techniques. Least-squares refinement can be carried out under most favourable circumstances (Dorset, 1995*a*), but requires the availability of a sufficient number of diffraction data. Even so, the refinement of thermal parameters must be uncoupled from that of the atomic positions. Also, positional shifts must be dampened (if X-ray crystallographic software is used) to prevent finding a false minimum, especially if the kinematical *R* factor is used as a figure of merit.

4.5.3.4. Examples of crystal structure analyses

At least four kinds of electron diffraction intensity data sets have been used as tests for direct phase determination *via* the approaches mentioned above.

Case 1: Zonal data sets – view down the chain axis. Such data are from the least optimal projection of the polymer packing, because of extensive atomic overlap along the chain axis. Initially, symbolic addition was used to find phase values for *hk*0 data sets from six representative polymers, including three complicated saccharide structures (Dorset, 1992). Most of the determinations were strikingly successful. Later, an unknown data set from the polysaccharide chitosan was obtained from Grenoble (Mazeau *et al.*, 1994) and direct phase determination was able to find a correct model (Dorset, 1995*b*). More recently, other polymers have been tested [including one case where an electron micrograph provided many of the starting phase terms (Dorset, 1995*b*)] also comparing favourably with the solution found by energy minimization of a linkage model. For all examples considered so far, the projected symmetry was centrosymmetric.

Later, it was found that a partial phase set provided by symbolic addition could be expanded to the complete zone by the Sayre equation (Dorset *et al.*, 1995). In all of these tests (Dorset, 1995*b*), there were only one or two examples where there were serious deviations from the phase terms found by other methods. Even in these instances, the potential maps could still be used as

Table 4.5.3.1. *Structure analysis of poly-γ-methyl-L-glutamate in the β form*

h0l	$\|E_h\|$	$\|F_o\|$	$\|F_c\|$	φ (°) (previous)	φ (°) (this study)
002	0.48	0.72	0.57	−63	−51
004	0.43	0.38	0.31	49	73
006	3.01	1.47	0.88	1	−3
100	1.48	2.12	2.37	0	0
200	1.03	1.04	1.06	0	0
300	0.30	0.65	0.89	0	0
400	0.35	0.15	0.46	0	0
500	0.23	0.07	0.04	180	180
101	0.75	1.02	0.67	−169	−178
201	0.32	0.31	0.42	90	108
102	0.42	0.48	0.56	17	14
202	0.40	0.33	0.64	41	43
103	0.95	0.85	0.77	88	90
203	0.51	0.36	0.42	91	88
303	0.12	0.06	0.31	92	87
403	0.13	0.04	0.54	90	90
104	0.66	0.45	0.27	−22	−13
105	0.55	0.28	0.29	−26	−7
106	1.75	0.69	0.58	5	−5

Fractional coordinates

	This study		Vainshtein & Tatarinova (1967)	
	x	*z*	*x*	*z*
Cα, β	0.048	0.000	0.042	0.000
C′	0.067	0.331	0.092	0.330
O	0.281	0.335	0.300	0.330
N	0.000	0.161	−0.025	0.175

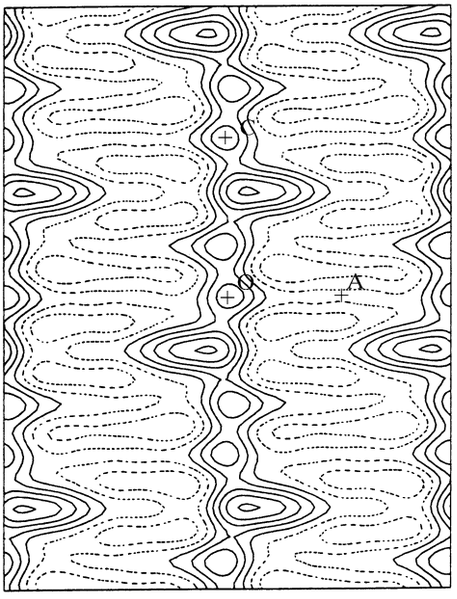

Fig. 4.5.3.1. Initial potential map for poly-γ-methyl-L-glutamate (plane group *pg*) found with phases generated by the Sayre equation.

envelopes for the actual projection of the chain structure (Dorset, 1992).

Case 2: Zonal data set – view onto the chain axes. Electron diffraction data from a projection onto the polymer chain axes would be more useful if individual atomic positions were to be resolved. An interesting example where such a view can be obtained is an *h0l* data set from the polypeptide poly-γ-methyl-L-glutamate. Electron diffraction data were collected from stretched films by Vainshtein & Tatarinova (1967). In projection, the cell constants are $a = 4.72$, $c = 6.83$ Å with plane-group symmetry *pg*. As shown in Table 4.5.3.1, there were 19 unique intensity data used for the analysis. After initial phase assignment by symbolic addition, a correct solution could be visualized which, after Fourier refinement (Dorset, 1995*b*), differed from the original one by a mean phase difference of only 6°.

The progress of this structure analysis can be reviewed to give a representative example. Since the *h*00 reflections have centrosymmetric phases, the value $\varphi_{100} = 0$ was chosen as a single origin-defining point. From high-probability Σ_1 three-phase invariants (assessed after calculation of normalized structure factors $|E_h|$), one could assign $\varphi_{200} = \varphi_{400} = 0$. Symbolic values were then given to three other phases, *viz.* $\varphi_{106} = a$; $\varphi_{103} = b$; $\varphi_{101} = c$. From this entire basis, other values could be found from highly probable Σ_2 three-phase invariants, as follows:

$$\begin{aligned}
\varphi_{006} &= \varphi_{106} + \varphi_{\bar{1}00} \;\;\therefore\;\; \varphi_{006} = a \\
\varphi_{105} &= \varphi_{006} + \varphi_{10\bar{1}} \;\;\therefore\;\; \varphi_{105} = a - c + \pi \\
\varphi_{203} &= \varphi_{106} + \varphi_{10\bar{3}} \;\;\therefore\;\; \varphi_{203} = a - b + \pi \\
\varphi_{300} &= \varphi_{100} + \varphi_{200} \;\;\therefore\;\; \varphi_{300} = 0 \\
\varphi_{002} &= \varphi_{103} + \varphi_{\bar{1}01} \;\;\therefore\;\; \varphi_{002} = b - c \\
\varphi_{004} &= \varphi_{006} + \varphi_{00\bar{2}} \;\;\therefore\;\; \varphi_{004} = a - b + c.
\end{aligned}$$

(These invariant relationships include phase interactions among symmetry-related Miller indices characteristic of the plane group.) Additionally $c = \pi$ could be specified to complete origin definition for the zone. It was then possible to permute values of *a* and *b* to arrive at test phase values for this subset, *i.e.* to generate a multiple set of solutions. When $a = 0$, $b = \pi/2$, the map in Fig. 4.5.3.1 was observed. After finding trial atomic positions for Fourier refinement (assuming that two carbon-atom positions were eclipsed in this projection), the final phase set was found as shown in Table 4.5.3.1. Although the crystallographic residual to the observed data, calculated with the model coordinates, was rather large (0.32), there was a close agreement with the earlier determination.

More recently a similar data set, collected from oriented crystal 'whiskers' of poly(*p*-oxybenzoate) in plane group *pg* was analysed. Again the Sayre equation, *via* a multisolution approach, was used to produce a map that contained 13 of 18 possible atomic positions for the two subunits in the asymmetric unit. The complete structure was observed after the remaining five atom sites were identified in two subsequent cycles of Fourier refinement (Liu *et al.*, 1997) and the average atomic positions were found to be within 0.2 Å of the model derived from an energy minimization.

Case 3: Three-dimensional data – single crystal orientation. The first data set from a chain-folded lamella for a direct structure analysis was a centrosymmetric set (space group $P2_1/n$) from poly(1,4-*trans*-cyclohexanediyl dimethylene succinate), composed of 87 reflections (Brisse *et al.*, 1984). The phase determination was quite successful and atomic positions could be found as somewhat blurred density maxima in the three-dimensional maps (Dorset, 1991*a*). A model was constructed from these positions and the bonding parameters optimized to give the best fit to the data ($R = 0.29$).

Noncentrosymmetric three-dimensional intensity sets (orthorhombic space group $P2_12_12_1$) from the polysaccharides mannan (form I) (Chanzy *et al.*, 1987) and chitosan (Mazeau *et al.*, 1994) were also collected from tilted crystals. In both cases, direct phase determination by symbolic addition *via* an algebraic unknown was successful, even though the data were not sampled along the chain repeat. For the former polymer, a monomer model could be fitted to the blurred density profile, much as one would fit a polypeptide sequence to a continuous electron-density map (Dorset & McCourt, 1993; Dorset, 1995*c*). If the Sayre equation were used to predict phases and amplitudes within the 'missing cone' of unsampled data, then the fit of the monomer could be much more highly constrained.

Case 4: Three-dimensional data – two crystal orientations. The optimal case for collection of diffraction data is when two

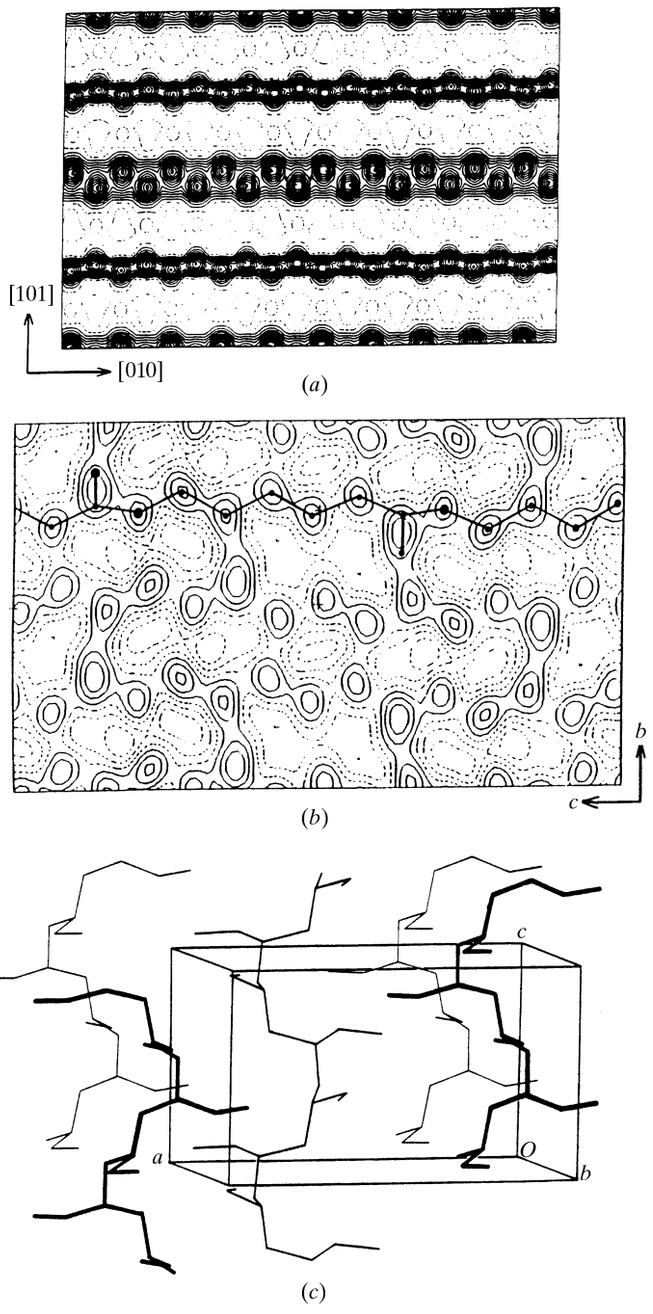

Fig. 4.5.3.2. Crystal structures of linear polymers determined from three-dimensional data. (*a*) Polyethylene; (*b*) poly(ε-caprolactone); (*c*) poly(1-butene), form (III).

orthogonal projections of the same polymer polymorph can be obtained, respectively, by self-seeding and epitaxic orientation. While tilting these specimens, all of reciprocal space can be sampled for intensity data collection.

Polyethylene crystals were used to collect 50 unique maxima (Hu & Dorset, 1989) and, *via* symbolic addition, the centrosymmetric phases of 40 reflections (space group *Pnma*) could be readily determined (Dorset, 1991*b*). The structural features were readily observed in the three-dimensional potential maps (Fig. 4.5.3.2*a*), and atomic coordinates (with estimated values for hydrogen-atom positions) could be refined by least squares (Dorset, 1995*b*) to give a final R value of 0.19.

Poly(ε-caprolactone) was epitaxically crystallized on benzoic acid and, with *hk*0 data from solution-crystallized samples, a unique set of 47 intensities was collected for the noncentrosymmetric orthorhombic unit cell (space group $P2_12_12_1$) (Hu & Dorset, 1990). Direct phase determination was achieved *via* symbolic addition, using one algebraic unknown to assign values to 30 reflections (Dorset, 1991*c*). Atomic positions along the chain repeat, including the carbonyl position, were clearly discerned in the [100] projection (Fig. 4.5.3.2*b*) and the three-dimensional model was constructed to fit to the map calculated from all phased data, yielding a final crystallographic residual R = 0.21. This independent determination was able to distinguish between two rival fibre X-ray structures, in favour of the one that predicted a nonplanar chain conformation. Because of the methylene repeat, this is actually a difficult structure to solve by automated techniques. For example, the tangent formula and *SnB* (Miller *et al.*, 1993) could only find chain zigzag positions and not the position of the carbonyl oxygen atom (Dorset, 1995*b*).

The most complicated complete polymer crystal structure solved so far by direct methods using electron diffraction data (Dorset *et al.*, 1994) was based on 125 unique data (space group $P2_12_12_1$) from isotactic poly(1-butene), form (III), using orthogonal molecular orientations crystallized in Strasbourg (Kopp *et al.*, 1994). Initially, the standard NQEST figure of merit (FOM) (De Titta *et al.*, 1975) was not suitable for identifying the correct solution among the multiple sets generated with the tangent formula. A solution could only be found when a separate phase determination was carried out with the *hk*0 data to compare with the multiple solutions generated. More recently, the minimal principle (Hauptman, 1993), used as a FOM with the tangent formula or with a multiple random structure generator, *SnB*, correctly identified the structure on the first try (Dorset, 1995*b*). The maps clearly show individual carbon-atom positions in a 4_1 helix that parallels 2_1 helices of the space group (Fig. 4.5.3.2*c*). After Fourier refinement, the crystallographic residual was R = 0.26. The previous powder X-ray diffraction determination was based on only 21 diffraction maxima, some of which had as many as 15 individual contributors.

The work of both RPM and DLD was supported by the US National Science Foundation (grant DBI-9722862 for RPM).

References

Alexeev, D. G., Lipanov, A. A. & Skuratovskii, I. Y. (1992). *Patterson methods in fibre diffraction. Int. J. Biol. Macromol.* **14**, 139–144.

Arnott, S. (1980). *Twenty years hard labor as a fibre diffractionist*. In *Fibre Diffraction Methods*, ACS Symposium Series, Vol. 141, edited by A. D. French & K. H. Gardner, pp. 1–30. Washington: American Chemical Society.

Arnott, S., Chandrasekaran, R., Millane, R. P. & Park, H. (1986). *DNA–RNA hybrid secondary structures. J. Mol. Biol.* **188**, 631–640.

Arnott, S. & Mitra, A. K. (1984). *X-ray diffraction analyses of glycosamionoglycans*. In *Molecular Biophysics of the Extracellular Matrix*, edited by S. Arnott, D. A. Rees & E. R. Morris, pp. 41–67. Clifton: Humana Press.

Arnott, S., Wilkins, M. H. F., Fuller, W. & Langridge, R. (1967). *Molecular and crystal structures of double-helical RNA III. An 11-fold molecular model and comparison of the agreement between the observed and calculated three-dimensional diffraction data for 10- and 11-fold models. J. Mol. Biol.* **27**, 535–548.

Arnott, S. & Wonacott, A. J. (1966). *The refinement of the crystal and molecular structures of polymers using X-ray data and stereochemical constraints. Polymer*, **7**, 157–166.

Atkins, E. D. T. (1989). *Crystal structure by X-ray diffraction*. In *Comprehensive Polymer Science*, Vol. 1. *Polymer Characterization*, edited by G. A. Allen, pp. 613–650. Oxford: Pergamon Press.

Barham, P. J. (1993). *Crystallization and morphology of semicrystalline polymers*. In *Materials Science and Technology. A Comprehensive Treatment*, Vol. 12. *Structure and Properties of Polymers*, edited by E. L. Thomas, pp. 153–212. Weinheim: VCH.

Baskaran, S. & Millane, R. P. (1999*a*). *Bayesian image reconstruction from partial image and aliased spectral intensity data. IEEE Trans. Image Process.* **8**, 1420–1434.

Baskaran, S. & Millane, R. P. (1999*b*). *Model bias in Bayesian image reconstruction from X-ray fiber diffraction data. J. Opt. Soc. Am. A*, **16**, 236–245.